



ARTICLE

Evaluation of the Antibacterial and Antifungal Capacity of Nanoemulsions Loaded with Synthetic Chalcone Derivatives Di-Benzyl Cinnamaldehyde and Benzyl 4-Aminochalcone

Flavia Oliveira Monteiro da Silva Abreu^{1,2,*}, Taysse Holanda¹, Joice Farias do Nascimento¹, Henety Nascimento Pinheiro¹, Rachel Menezes Castelo¹, Hécio Silva dos Santos³, Thais Benincá⁴, Patrícia da Silva Malheiros⁴, Júlio César Sousa Prado⁵, Raquel de Oliveira Fontenelle⁵ and Maria Madalena de Camargo Forte²

¹Natural Polymers Laboratory, PPGCN, State University of Ceará, Fortaleza, 60.714.903, Brazil

²Polymeric Materials Laboratory, PPGE3M, Federal University of Rio Grande do Sul, Porto Alegre, 91501-970, Brazil

³Natural Product Chemistry Laboratory, PPGCN, State University of Ceará, Fortaleza, 60.714.903, Brazil

⁴Food Hygiene and Microbiology Laboratory, PPGCTA, Federal University of Rio Grande do Sul, Porto Alegre, 91501-970, Brazil

⁵Microbiology Laboratory, Medicine School, Federal University of Ceará, Sobral, 62010-560, Brazil

*Corresponding Author: Flavia Oliveira Monteiro da Silva Abreu. Email: flavia.monteiro@uece.br

Received: 16 July 2023 Accepted: 02 September 2023 Published: 11 March 2024

ABSTRACT

With the increase in antimicrobial resistance, it has become necessary to explore alternative approaches for combating and preventing diseases. DB-cinnamaldehyde (CNM) and Benzyl4-amino (B4AM) are bioactive compounds derived from chalcones but with restricted solubility in aqueous media. Nanoemulsions can enhance the solubility of compounds and can be a promising alternative in the development of novel antimicrobials, with reduced side effects and prolonged release. The objective of this study was to evaluate the stability of oil-in-water nanoemulsions loaded with two distinct types of chalcones at two different dosages, to propose a stable formulation with antimicrobial properties. Results showed that nanoemulsions presented high encapsulation efficiency, low polydispersity index (PDI) and particle size below 200 nm, indicating that emulsification was a suitable method for nanoemulsion preparation. Nanoemulsions with higher dosages exhibited significant antimicrobial effects when compared to free chalcones and positive controls. Notably, B4AM nanoemulsions at higher dosages showed expressive activity against *Salmonella minnesota*, with a 420% greater inhibitory response compared to the free form and showing equivalence to the positive control. CNM nanoemulsions showed excellent inhibitory activity at the highest dosage, equivalent to the positive control against *S. minnesota* and *Staphylococcus aureus*. The greater number of conjugated bonds in CNM increased the antimicrobial activity in comparison with B4AM, and the formation of nanometric domains enhanced the bioavailability, being a promising alternative for antimicrobial applications.

KEYWORDS

Polysaccharide; nanoemulsions; *S. aureus*; *S. minnesota*; chalcones; alginate



Nomenclature

CNM	DB-cinnamaldehyde
B4AM	Benzyl4-amino
PDI	Polydispersity Index

1 Introduction

Salmonella belongs to the Enterobacteriaceae family and is one of the main food-borne pathogens in the world [1]. This bacterium can be found in a wide variety of hosts [2] and in a wide variety of foods, including eggs, poultry, swine and cattle, and raw milk, which are the major foods involved in outbreaks of this pathogen [3]. *Staphylococcus aureus* is a spherical bacterium, from the group of gram-positive cocci, frequently found in the skin and nasal cavities of healthy people. This pathogen can cause a wide variety of diseases, ranging from moderately severe skin infections to potentially fatal pneumonia and sepsis [4]. Despite the availability of various antibiotics to combat this pathogen, the constant emergence of *S. aureus* strains that are resistant to each new antibiotic introduced for treating related conditions causes the development of alternative approaches to conventional antibiotics [5]. *Candida albicans* is a kind of fungus present in the microbiota of the human body, but it is a pathogen when the patient's immune system is in decline and causes superficial infections, mainly in mucous membranes, but can cause invasive infections, common in hospitalized patients [6], leading to the risk of death [7].

Bacterial cells are polarized, and the membrane potential is an important energy source for respiration, nutrient uptake, and toxin export. Membrane depolarization and hyperpolarization have been suggested to be primary indicators of injured bacteria [8]. Antimicrobial drugs inhibit or interfere in the peptidoglycan's synthesis layer, an important component of the bacterial cell wall. The fungal cell wall is not affected by antibacterial cell wall inhibitors. Antifungal agents can work through different mechanisms, mainly by cell membrane disruption, inhibition of cell division or inhibition of cell wall formation [9].

Studies have demonstrated the great pharmacological potential of chalcones, which have been researched because of their relatively simple structure and the diversity of pharmacological activities, such as antimicrobial [10,11] and anti-inflammatory [12] activity, among others. Chalcones are naturally occurring aromatic ketones abundantly found in plants from the *Leguminosae*, *Compositae* and *Moraceae* families, belonging to the class of open-chain flavonoids [13]. The antimicrobial effects are because of reactions between these compounds and the cell membrane of the target microorganism [11]. However, as they are lipophilic organic compounds, they have restricted solubility in aqueous media, which hinders and restricts their pharmacological applications [14].

The development of nanoemulsions of biodegradable polymers for controlled release systems of several active principles has been promising, since such systems can present a better performance compared to conventional administration, with reduced side effects and prolonged effectiveness [15]. Nanoemulsions are dispersions of kinetically stable immiscible components stabilized by a surfactant, forming a nanoscale colloidal material that can be used for the encapsulation of bioactive compounds [16]. They range in size from 10 to 200 nm, and their small size provides advantages such as greater surface area and stability [17,18]. Long-chain triglycerides (LCT) comprise a wide variety of oils which contain fatty-acid chains longer than 12 carbons [19]. Olive oil and corn oil were added to glyceryl trioctanoate to form nanoemulsions and showed an improvement in the physical stability of nanodroplets by limiting the Ostwald ripening rate [20]. However, Soybean oil is a LCT with low cost largely produced in Brazil and other countries [21]. Nanoemulsions prepared by spontaneous emulsification or high-pressure homogenization with Soybean oil, Medium-chain triglycerides and Egg-yolk lecithin showed high stability when prepared by high pressure homogenization [19]. Nanoemulsions containing polymeric matrices stand out among the encapsulation systems because of their amphiphilicity, high solubility and

permeability in water, biocompatibility, and tensile strength [22,23]. To improve the biocompatibility and biodegradability of the carrier system, there is a tendency to use polymers based on natural polysaccharides [24]. Alginate is a water-soluble polysaccharide over a wide range of pH and temperature, producing a thickening and/or gelling effect. Sodium alginate is composed of mannuronic (M) and guluronic (G) acid sequences and forms a gel in the presence of divalent cations because of the formation of bridges between the chains, constituting an anionic polysaccharide [25]. Polysaccharides can act as stabilizers, by the thickening of the aqueous phase, or even can act as emulsifiers, where the chain can absorb to the surface of freshly formed droplets of an oil-water interface during homogenization, forming a protective membrane that prevents the droplets from aggregating. These factors can contribute to the increase of the emulsion's stability [26].

Nanomaterials can bind in components of bacterial cells, such as DNA, ribosomes, and enzymes, and disrupt normal physiological activities of the cell, resulting in the oxidative stress, electrolyte imbalance, enzyme inhibition and other bacteriostatic effects, and ultimately leading to cell death [9,27].

Nanoemulsions containing chalcones or chalcone-based compounds have been produced in the last 10 years to evaluate their pharmacological potential, such as antimoral [28], anthelmintic [29,30], antimicrobial [31] and antifungal [32]. Nanoemulsions with synthetic chalcones were developed as a topical formulation to treat cutaneous leishmaniasis [29,30]. Other study investigated the antimicrobial activity of synthetic chalcones in the increase of potential activity of Norfloxacin against *S. aureus* [31]. Another study evaluated the activity of 2-hydroxychalcone-loaded in nanoemulsion against *Paracoccidioides brasiliensis* and *Paracoccidioides lutzii*, showing high antifungal activity, high selective index value and lack of cytotoxicity *in vitro* [32]. However, to the best of our knowledge, nanoemulsions based on di-benzyl cinnamaldehyde (CNM) and benzyl-4-amino-chalcone (B4AM) for the inhibition of *S. aureus*, *S. minnesota* and *Candida albicans* have not yet been developed. Therefore, the objective of this study was to evaluate the inhibitory capacity of DBCNN and B4AM free and carried in alginate nanoemulsions in different dosages against *S. minnesota*, *S. aureus* and *C. albicans*.

2 Materials and Methods

2.1 Materials

Sodium alginate (DINÂMICA), Tween 80[®] surfactant (VETEC), dihydrated calcium chloride (Dinâmica), and commercial soybean oil were used. The synthetic chalcones (1E,3E,6E,8E) 1,9-diphenyl none-1,3,6,8-tetraen-5-one (CNM, 286 g/mol) and (E)-1-(4-(dimethyl-amino) phenyl) but -2-en-1-one (B4AM, 189,12 g/mol) were produced and provided by the UECE Natural Products Chemistry Laboratory.

2.2 Synthesis of Chalcones

The synthetic chalcone (E)-1-(4-(dimethyl-amino) phenyl) but-2-en-1-one (B₄AM) was obtained by Claisen-Schmidt condensation, as described by Romeu [33]. Similarly, (1E,3E,6E,8E) 1,9-diphenylnone-1,3,6,8-tetraen-5-one (CNM), was obtained by controlled addition of 7 mL of benzaldehyde: acetone (5:2), in a mixture of 50 mL KOH 10%(w/v) and 40 mL of ethanol. The reaction was kept under mechanical stirring at room temperature, and after 30 min the mixture was filtered, and the precipitate was washed with distilled water. The compound was recrystallized using ethanol as solvent.

2.3 Methodology

Four distinct nanoemulsions were prepared where the type of chalcone and the concentration of chalcone inserted in the emulsion were varied, keeping the surfactant content in a 1:1 (v/v) proportion in relation to soybean oil (SO) and calcium chloride constant in relation to the polymer matrix (1:15) (v/v). The nanoemulsions preparation was prepared by ultrasound, where in a 50 mL falcon tube, 15 mL of the 1% polymeric matrix solution was added. In the oil phase, different dosages of chalcone B4AM and

CNM were added to 300 μL of DMSO and 300 μL of soybean oil, and then homogenized in a sonicator tip for 30 s. The oil phase was poured with the aid of a syringe into the aqueous phase, where it was homogenized in a sonicator with a tip at an ultrasonic frequency of 20 KHz at a Power of 160 W for 2 min. Finally, 0.5% calcium chloride was added as a thickening agent, and the nanoemulsion was stirred by ultrasound for another 1 min.

2.4 Characterizations

The stability of the nanoemulsions was carried out through visual analysis of the samples in the period from 7 to 21 days, where the appearance of creaming or sedimentation was verified. Optical microscopy was performed using a Carl Zeiss Axioscope A1 optical microscope, where a drop of each formulation was deposited on a slide and covered with a coverslip. The morphology of the samples was visualized with a 20x objective.

Droplet size, polydispersity index (PDI) and zeta potential from nanoemulsions were determined after 15 days by dynamic light scattering using the Malvern Zetasizer equipment (Malvern Instruments). The nanoemulsions were dispersed in distilled water, forming a concentration of 1% (v/v) in water and left in agitation for 12 h to ensure full matrix dispersion in an aqueous medium. Chalcones and Nanoemulsions were characterized by infrared spectroscopy (FTIR) on a Nicolet iS5 model (Thermo Scientific).

2.5 Encapsulated Chalcone Content

The nanoemulsions code produced, the drug loading and the calculated encapsulation efficiency are given in [Table 1](#).

Table 1: Nanoemulsions code according to the chalcone type and theoretical and experimental loading with the respective encapsulation efficiency (%EE). The drug loading was calculated by the amount of chalcone added to the total volume of the reaction media

Nanoemulsions code	Chalcone type	Ratio drug surfactant	Drug loading (mg/mL)	%EE
15CNM	CNM	1:14	1.45	103.4 \pm 9.0
15BAM	B4AM	1:14	1.45	95.1 \pm 2.99
45CNM	CNM	1:4	4.50	100.5 \pm 1.43
45BAM	B4AM	1:4	4.50	92.1 \pm 2.07

The encapsulation efficiency of chalcones B4AM and CNM was determined by placing 1 mL of each emulsion in 4 mL of ethanol (96%) and allowing it to stand for 24 h. After the phase separation, 1 mL of the ethanolic phase was withdrawn, diluted to 3 mL with ethanol 96% and taken for reading in the Kazuaki Spectrophotometer (GENESYS 6 UV-Vis) at a wavelength of 289 nm. Further dilutions until a factor of 100 x were taken place to fit the absorbance into the calibration curve, to ensure the linearity between absorbance and concentration. The chalcone content in the nanoemulsions was determined through a calibration curve, prepared in triplicate in a standard solution of 150 mg/L of B4AM e CNM in ethanol 96% (Dinâmica). Further dilutions were made to obtain concentrations from 75 to 1 mg/L. The calibration curve for chalcones B4AM and CNM are represented, respectively, by [Eqs. \(1\)](#) and [\(2\)](#):

$$y = 0.0901 \times - 0.0061 \rightarrow R^2 = 0.9993 \quad (1)$$

$$y = 0.0344 \times + 0.0198 \rightarrow R^2 = 0.9928 \quad (2)$$

The accuracy of the encapsulation efficiency determination might be affected because of high dilution, leading to fluctuations. Duplicate tests were performed. Eq. (3) was used to determine the Encapsulation Efficiency (%EE) value.

$$\%EE = \frac{\text{Determined chalcone content}}{\text{Total theoretical chalcone content}} \quad (3)$$

2.6 Antibacterial and Antifungal Susceptibility

The *S. aureus* (ATCC 1901) and *S. minnesota* (7.301.007) strains were grown in BHI broth at 37°C for 18 to 24 h. Adjusting the suspension to a concentration of 8 log CFU/mL resulted in an optical density of 0.5 (OD 630 nm) in the spectrophotometer (Ultrospec Tm 3100 Pro–Ge, Healthcare England). Then, it was readjusted to a concentration of 6 log CFU/mL through decimal dilutions. The inoculum was seeded by introducing a sterile swab into the bacterial suspension and spreading it over the surface of sterile plates containing BHI agar in three different directions. Then, 10 µL of nanoemulsions were inoculated. Plates were incubated upside down at 37°C for 18 to 24 h [34].

The *C. albicans* (ATCC 90028) and (LABMIC 0102) strains were cultivated in Mueller-Agar (HIMedia) and used according to directions. The antibacterial and antifungal activity was also evaluated for free chalcones by dissolving each chalcone in DMSO forming a 1.5 mg/mL solution. ALG nanoemulsions produced without chalcones were used for negative control, and for positive control, sulfamethoxazole 100 µg/mL + trimethoprim 20 µg/mL and Nistatin 100 U.I. were used. Results were read by observing the presence and/or absence of zones of inhibition for the evaluated compound. The inhibitory zone was measured in millimeters using photographs with scale and the Image J software, version 1.53t.

The compounds' minimum inhibitory concentration (MIC) was determined regarding *C. albicans* strains were determined by the broth microdilution method, using 96-well plates according to the CLSI M27-A3 document [34]. A serial dilution covering the concentration range of 0.0024–2.50 mg/mL⁻¹ in an RPMI 1640 medium with L-glutamine (pH 7.4) was prepared from the compound's stock solution. Amphotericin B was used as a standard drug control between 0.015–16 µg mL⁻¹.

3 Results and Discussion

Two types of chalcones were encapsulated as nanoemulsions to evaluate the effect of the structure of the compounds and the presence of amino groups in relation to their antimicrobial potential. The effectiveness of nanoemulsion formulations composed by non-ionic surfactant Tween 80, soybean oil as co-surfactant and using sodium alginate as stabilizer agent was evaluated at two different dosages: 1.5 mg/mL and 4.5 mg/mL. Regarding interfacial tension, triglycerides from vegetable oils such as corn and soybean can concentrate on the oil-water interface of the micelle, competing with other surfactants, and thus further decreasing interfacial tension [20]. All formulations presented high encapsulation efficiency (see Table 1), indicating that the emulsification was a suitable method for nanoemulsion preparation. Our results indicate that with a chalcone/surfactant mass ratio of 1:4 a PDI of less than 0.3 and a particle size of less than 100 nm was achieved compared to those with a chalcone/surfactant mass ratio of 1:14. The high values of EE (>80%), observed for the nanoemulsions with both chalcones, can be explained by the higher affinity of the molecules to the oily phase within the droplets than to the aqueous solution phase during the preparation process, corroborating with the other authors [28]. In the work of Kim et al. [35], a chalcone derivative was entrapped in droplets using a monomethoxy poly (ethylene glycol)-poly(D,L-lactide), where their findings indicated that changing the drug/surfactant mass ratios influenced the properties of resultant nanoparticles, with optimal results with 1:5 drug:surfactant mass ratio.

3.1 Analysis of the Functional Groups of Chalcones and Nanoemulsions by FTIR

The functional groups of chalcones and nanoemulsions were investigated through FTIR spectroscopy, which is shown in Fig. 1. The broad absorption band characteristic of ALG is present at 3390 cm^{-1} , referring to the OH stretching of the polysaccharide chain [24,25]. An asymmetric band at 1610 cm^{-1} and a narrower symmetric band at 1414 cm^{-1} are attributed to stretching of the CO-O-O bond and axial stretching of the carboxylic ion, respectively. An even wider absorption observed near 1098 cm^{-1} can be attributed to COH stretching. These absorption bands are under the literature [36–38].

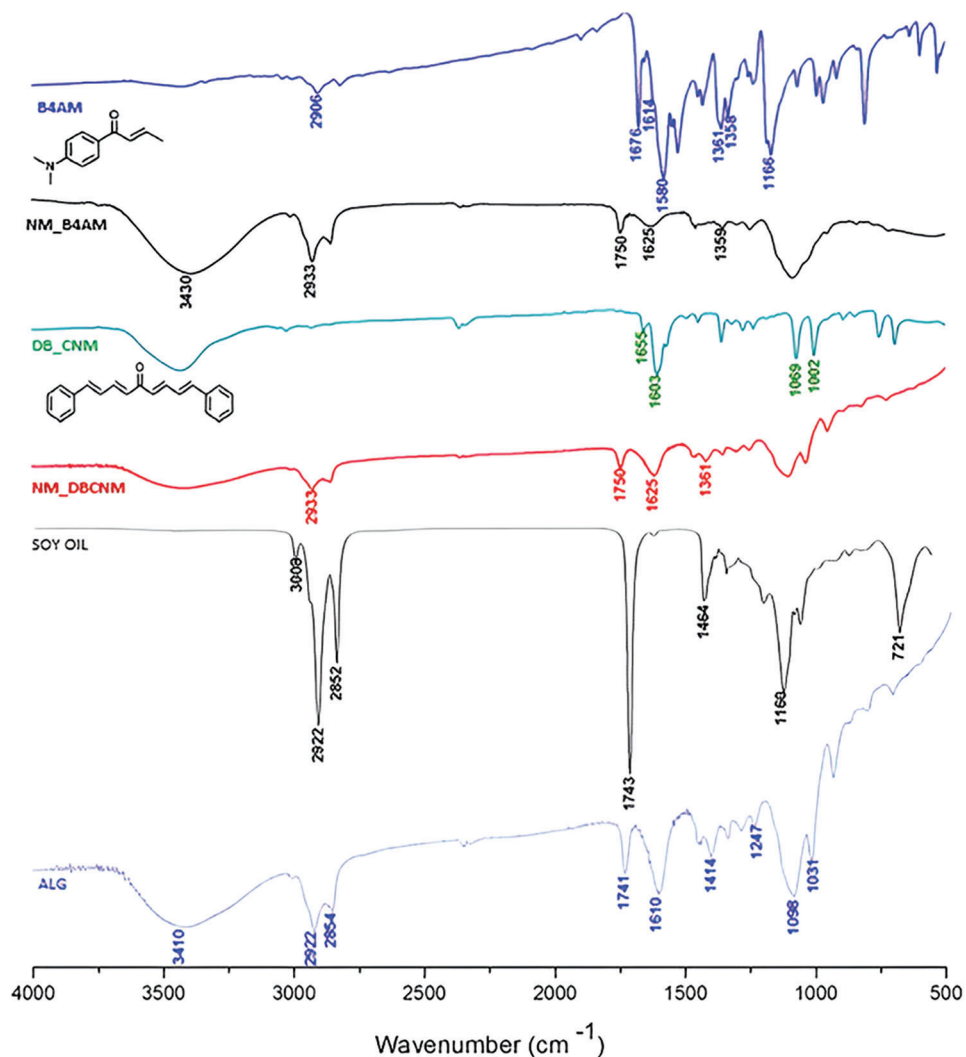


Figure 1: FTIR from the free chalcones, the components ALG and soybean oil and the nanoemulsions with CNM and B4AM

Soybean oil presents main vibration modes at 3009 cm^{-1} attributed to $=\text{C-H}$ (cis) stretching. The bands at 2922 and 2852 cm^{-1} represent the asymmetric and symmetric stretching of (CH_2) , and $-\text{C-H}$ (CH_2) Bending (scissoring) is displayed at 1463 cm^{-1} . At 1743 cm^{-1} , the $-\text{C=O}$ bond displays the strongest ester stretch and at 1160 cm^{-1} , the $-\text{C-O}$ bond demonstrates the stretch. The bending out of plane for cis-CH=CH- is represented by the peak at 722 cm^{-1} , according to [39].

Chalcone B4AM presents a broad medium intensity infrared band at 3448 cm^{-1} attributed to the NH_2 anti-symmetric stretching mode [40]. The stretching modes involving the CH_3 group are found at 2906 cm^{-1} and the carbonyl $\text{C}=\text{O}$ stretching bands are found at 1676 cm^{-1} superimposed on the $\text{C}_\alpha\text{-C}_\beta$ stretching vibrations.

At 1614 cm^{-1} , there are carbon-carbon stretching modes combined with $\text{C}_\alpha\text{-C}_\beta$ stretching are because of the conjugation effect, according to Santiago et al. [41]. The vibrational mode at 1580 cm^{-1} corresponds to a mixture of the C-N stretching mode with modes associated with displacements of HCC atoms. Chalcone CNM presents carbonyl $\text{C}=\text{O}$ stretching bands in lower wavenumber, at 1655 cm^{-1} , superimposed on the $\text{C}_\alpha\text{-C}_\beta$ stretching vibrations, which are the unsaturated carbons connecting the rings. This effect results from the increase in the conjugation effects that increase the single bond character of the $\text{C}=\text{O}$ and $\text{C}=\text{C}$ bonds in the resonance hybrid and hence lower their force constants, resulting in a lowering of the absorption frequencies, corroborating with results from [42]. The bands at 1603 cm^{-1} correspond to stretching modes associated with the $\text{C}_\alpha\text{-C}_\beta$ carbons, and the bands at 1102 cm^{-1} and 1069 cm^{-1} originate from CC stretching modes associated with deformations of BCC atoms in the aromatic rings.

Within the nanoemulsions, a double peak was detected between 2933 to 2852 cm^{-1} , which was attributed to the CH_2 stretching from ALG and soybean oil. The soybean oil ester peak was observed at 1750 cm^{-1} . The band at 3430 cm^{-1} for NM_B4AM is attributed to the NH_2 anti-symmetric stretching mode from the amino group from B4AM combined with the OH- stretching from ALG. For NM_CNM, the broader band with peak at 1625 comprehends the overlapping of peaks 1655 and 1603 cm^{-1} from CNM, and 1610 cm^{-1} from ALG groups. In summary, Nanoemulsion peaks are superimposed with the free chalcones, ALG and soybean oil, being preponderant of the stretching and vibrations present in the ALG polysaccharide and soybean oil.

3.2 Physical Stability

The physical stability of chalcone nanoemulsions with ALG was studied by changes in gravitational separation, particle size, zeta potential, and microstructure.

3.2.1 Creaming and Sedimentation

The physicochemical stability of nanoemulsions is characterized as kinetically stable systems, as these break down over time due to destabilizing physical mechanisms [18]. Creaming is defined as the upward movement of droplets because of their lower density in comparison with the surrounding liquid, whereas sedimentation is the downward movement of droplets because of their higher density than the surrounding liquid [43]. Nanoemulsions were observed regarding creaming and sedimentation (Fig. 2). Preliminary results showed that nanoemulsions with only tween and the chalcone are unstable, with flocculation points and sedimentation after seven days. Nanoemulsions with soybean oil, chalcone and tween minimized flocculation, however formed creaming. The addition of ALG in the nanoemulsion minimized creaming formation (Fig. S1 and Table S1, Supplementary Materials).

Creaming index was measured over 28 days (Fig. 2a). Nanoemulsions with a dosage of 1.5 mg/mL showed less than 2.5% of creaming even after 21 days, showing good stability. With the increase of the dose of chalcone to 4.5 mg/mL , there was a distinct behavior; the nanoemulsion DB4_4.5 presented an even higher stability, with a lack of creaming (Fig. 2a), but showed 4.0% sedimentation (Fig. 1b). Nanoemulsion CNM_4.5 showed an increasing creaming index to 3.8% (Fig. 1a), and the lack of sediment formation (Fig. 2b). Alginate used as an emulsion stabilizer may increase the kinetic stability of emulsions by modifying the rheological properties of the oil phase or by adsorption at the oil-water interface, thus providing an electrosteric barrier [26]. In another study, Salvia-Trujillo et al. [44] stated that lipid droplets coated by a non-ionic surfactant (Tween 80) and alginate do not show a powerful attraction between the polysaccharide and the droplet surfaces. However, at higher alginate concentrations

(1%), the aqueous phase viscosity increases and slows down the ascendant movement of droplets, which reduces creaming. In our study, alginate was probably acted by modifying the rheological properties of the oil phase, retarding the upward movement of droplets. However, there was some sediment formation for nanoemulsions DB4_4.5 and CNM_1.5. As already described by several authors [44–46] non-adsorbed polysaccharides can promote droplet aggregation in emulsions through a depletion mechanism at intermediate concentrations, leading to a small degree of flocculation. Other study [45] discussed that small amounts of highly extended polysaccharide molecules induce depletion and flocculation in aqueous solutions.

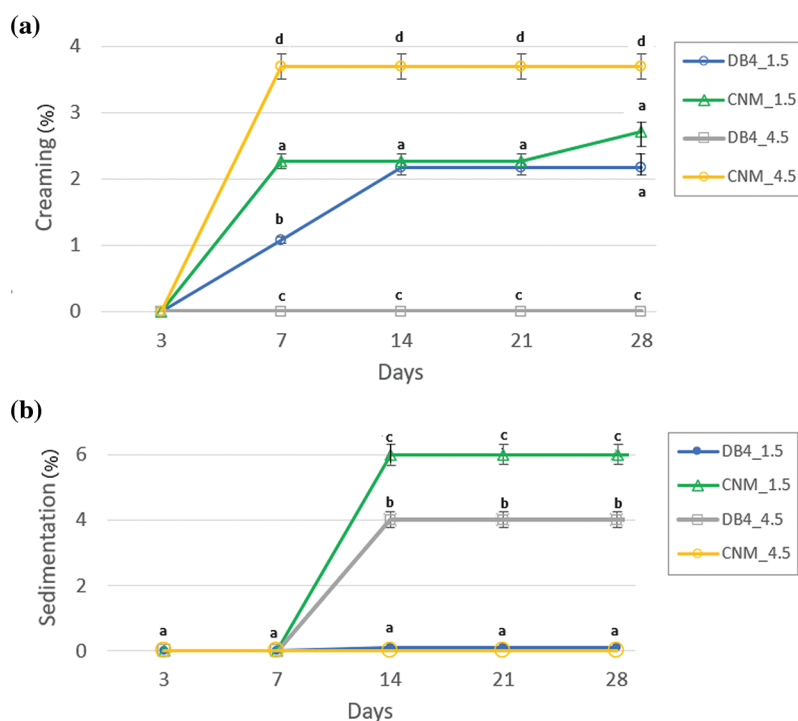


Figure 2: (a) creaming index and (b) sedimentation index as a function of the period of analysis for nanoemulsions of alginate with chalcones B4AM and CNM at different dosages

In summary, there is a need to conduct a very careful balance in the alginate content. If a higher amount of alginate increases the aqueous viscosity and prevents the ascendant movements of the droplets for creaming, a small excess of non-adsorbed polysaccharide in the dispersion medium may cause depletion mechanism and cause flocculation of the nanoemulsion. Considering that a nanoemulsion is a metastable system and subject to a variety of destabilization mechanisms [46], our stability results indicate nanoemulsions with low creaming and low sedimentation values.

3.2.2 Microstructure

It was observed that the CNM emulsions presented nanodroplets with relatively uniform size, with some domains of micrometer size (Figs. 3a and 3b). It is also perceptible the presence of some agglomerated domains, particularly for the CNM_4.5. As for the B4AM emulsions (Figs. 3c and 3d), nanoparticles with more uniform domains were observed for both types of dosage, where B4AM_4.5 showed very dispersed particles with nano-sized dimensions.

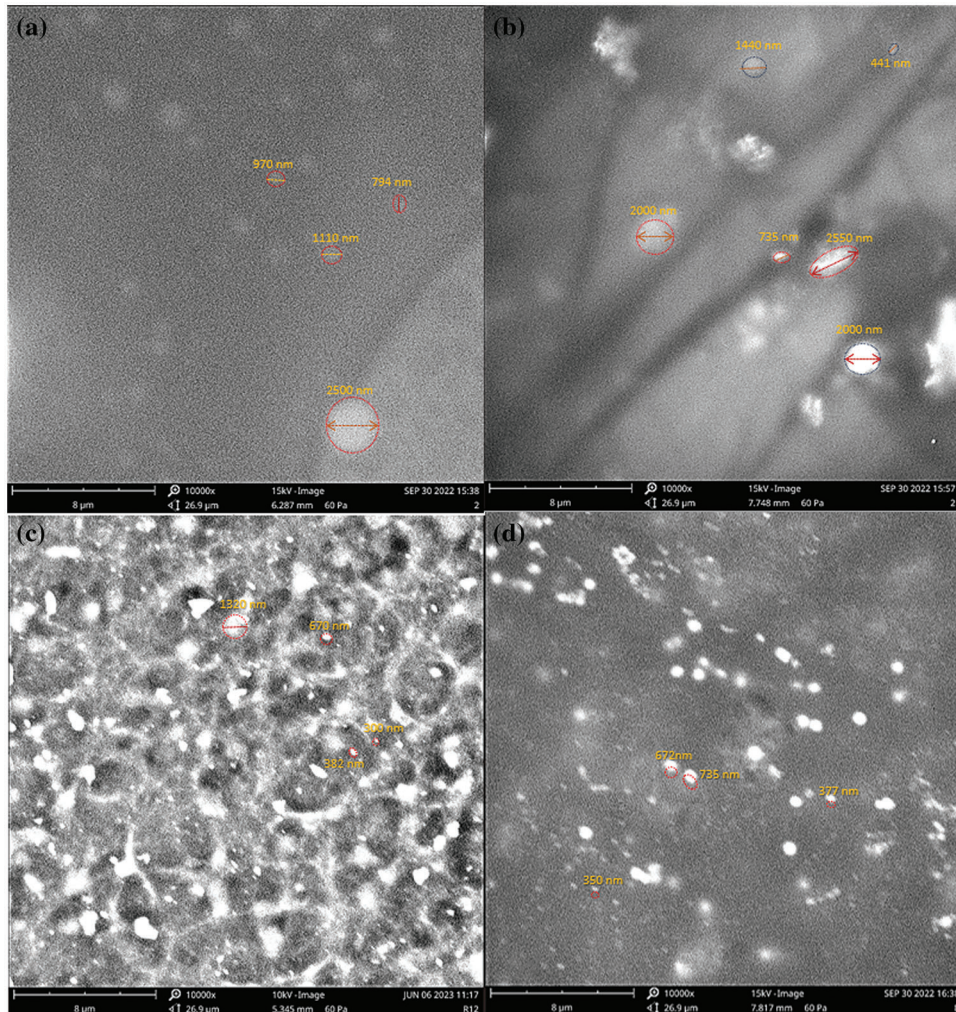


Figure 3: Scanning electron microscopy for ALG Nanoemulsions loaded with chalcones at 10.000×: (a) CNM_1.5; (b) CNM_4.5; (c) B4AM_1.5 and (d) B4AM_4.5

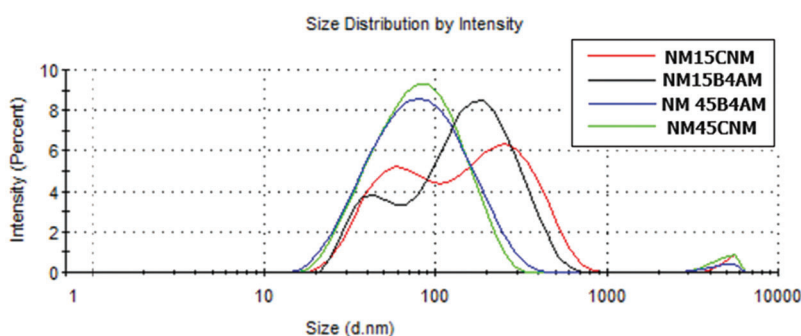
Anise oil-based nanoemulsion were developed and exhibited in SEM images of particles with a spherical shape and micrometric size [47]. Hassanshahian et al. [48] developed chitosan nanoemulsions loaded with *Alhagi maurorum* presented spherical nanoparticles with monomodal distribution. Our results showed a profile where B4AM nanoemulsions showed uniform nanoparticles and CNM nanoemulsions presented higher size dispersion because of the agglomerated particles. These results are according to the creaming analysis, once creaming is a sign of instability, therefore they are more likely to show an increase in droplet size because of aggregation of particles.

3.2.3 Particle Size and Zeta Potential

The nanoemulsions showed variation in micelle particle size and surface charge values according to the reaction condition. Table 2 shows the Polydisperse Index (PDI), Particle Size and zeta potential values for nanoemulsions loaded with B4AM and CNM. Size distribution by intensity for nanoemulsions of alginate with chalcones B4AM and CNM at different dosages is shown in Fig. 4.

Table 2: Nanoemulsions code, polydispersity index (PDI), particle size average values, and zeta potential values

Code	PDI	Particle size (nm)	Zeta potential (mV)
NM15CNM	0.445 ^a	202.8 ± 100 (63%) ^a 51.4 ± 16 (34%)	-35.6 ± 5 ^a
NM15B4AM	0.364 ^b	192.8 ± 93 (80%) ^a 42.49 ± 16 (19%)	-40.5 ± 5 ^b
NM45CNM	0.256 ^c	89.75 ± 50 ^b	-27.2 ± 7 ^c
NM45B4AM	0.261 ^c	94.9 ± 60 ^b	-32.7 ± 8 ^a

**Figure 4:** Size distribution by intensity for nanoemulsions of alginate with chalcones B4AM and CNM at different dosages

The particle size defines whether the formulations are in the nanometric range and may affect the penetration of the active substance through the membrane or bacterial cell [49]. Nanoemulsions loaded with 1.5 mg/mL presented droplets with a multimodal distribution pattern. There is a first peak with a size around 50 nm and medium intensity (19–34%), a second peak with a size around 200 nm and high intensity (63–80%) and a third peak with a size around 5000 nm, representing only from 1% to 3% of the total intensity. Nanoemulsions loaded with 4.5 mg/mL presented a bimodal distribution, with the main peak around 90 nm with high intensity (98%), and a second peak with an average size around 5000 nm (2%). All nanoemulsions presented the main peak with nano-sized dimensions, however, nanoemulsions produced with lower chalcone content presented a fraction with a size lower than 50 nm, which may enhance pharmacological properties. A study about the effect of particle size and surface charge of nanoparticles in penetration through intestinal mucus barrier showed that particles with 50 nm diameter showed the greatest permeation in comparison with those with 200 nm diameter [50].

Regarding the effect of the variables on the particle size, the nanodroplets presented a diameter ranging from 89 to 203 nm. PDI values ranged from 0.256 to 0.445. It should be noted that, according to McClements [46], any discrepancy between the size of particles evaluated at SEM measurements and by light scattering is attributed to the fact that any aggregation of particles caused by flocculation in an emulsion that is held together by osmotic attraction are usually dissociated when the sample is diluted for particle size measurements.

Nanoemulsions loaded with 4.5 mg/mL resulted in statistically significant lower particle size ($p < 0,05$), and lower PDI compared with those loaded with 1.5 mg/mL (Table S2) The higher dosage of chalcone

probably increased the attractive interactions within the droplet, resulting in a more compact droplet. Nanoemulsions loaded at 1.5 mg/mL have a higher soybean oil content relative to chalcone (15:1) compared to those loaded at 4.5 mg/mL (5:1). Considering that long-chain triglycerides can increase droplet size over time, with a lower soybean oil content, it may favor greater stability of nanoemulsions with smaller size and lower polydispersion index [20]. In another study, it was found that the replacement of at least 50% of the oil phase by high molar volume insoluble long-chain triglycerides provides a kinetic barrier to the phenomenon of coalescence and makes them more insoluble and thermodynamically stable [50]. Another explanation for why a smaller amount of soybean oil was more effective is because the emulsification occurred via ultra-sonication. Considering that this is a high-energy emulsification technique, a lower triglyceride content can cause the same barrier effect, since the method requires a low concentration of emulsifier compared with other mechanical methods [51]. In the work by Dan et al. [13], five different essential oils had a particle size of 90 to 160 nm, and the differences were attributed to the composition of the oil phase, corroborating the results of our study.

However, all nanoemulsions in this study had a droplet size equal to or less than 200 nm, and PDI index values below 0.500, which according to McClements [43] provided long kinetic stability, which can protect against droplet aggregation and gravitational separation, contributing to increase the long-term stability of the formulation.

High module zeta potential increases the distance and electrical repulsion between the particles. Nanoemulsions presented zeta values from -27 mV to -40 mV, as shown in Table 2. These negative values are characteristic of excellent electronic stabilization and are related to the carboxyl groups of the ALG, which coat the droplets.

However, there was a statistical influence ($p < 0.05$) of the dosage on the particle zeta potential values, where nanoemulsions produced with a dosage of 4.5 mg/mL, therefore with lower surfactant content presented lower zeta potential than the ones with 1,5 mg/mL (Table S3). Here, the effect is attributed to the amount of Tween 80 in the droplet. Sorbitan mono-oleate nanoemulsions with negative values have been attributed to the free fatty acids from MCT, and from the adsorption of hydroxyl ions at the oil-in-water interface with the subsequent development of hydrogen bonds between these ions and ethylene oxide groups of Tween [52–54]. With the increase of surfactant: drug content in the nanoemulsion from 4:1 to 14:1, there is a significant increase in the number of molecules of Sorbitan mono-oleate in the nanoemulsion, which favors the increase in the number of interactions of ethylene oxide groups with the hydroxyl ions, leading to a higher contribution of the surfactant in increasing the zeta potential values.

All zeta potential values, such as those found in this study, are characteristic of excellent electronic stabilization. This result indicates that NEs present stability where ALG successfully coated the surface of droplets, formed by chalcone in the inner core, and the sorbitan mono-oleate may contribute with charges when added in significantly higher amount, with the vegetable oil in the micellar interface.

3.3 Evaluation of the Antimicrobial Activity of Nanoemulsions

Encapsulation of chalcones is important in improving physicochemical conditions and bioavailability, optimizing a controlled release. Alginate is one of the most widely used polysaccharides for nanoemulsions. Nanoemulsions, because they are prepared by the oil-in-water method using ultrasound without the presence of harmful substances, are considered a safe method. Regarding their antimicrobial activity against *S. minnesota*, the results measured of the inhibition zones in diameters are shown in Fig. 5a. When there is no halo formation, it indicates that the substance could not prevent the growth of microorganisms. Larger halo diameters characterize its antimicrobial potential. The results showed that free chalcones showed differentiated antimicrobial activity depending on the type of microorganism.

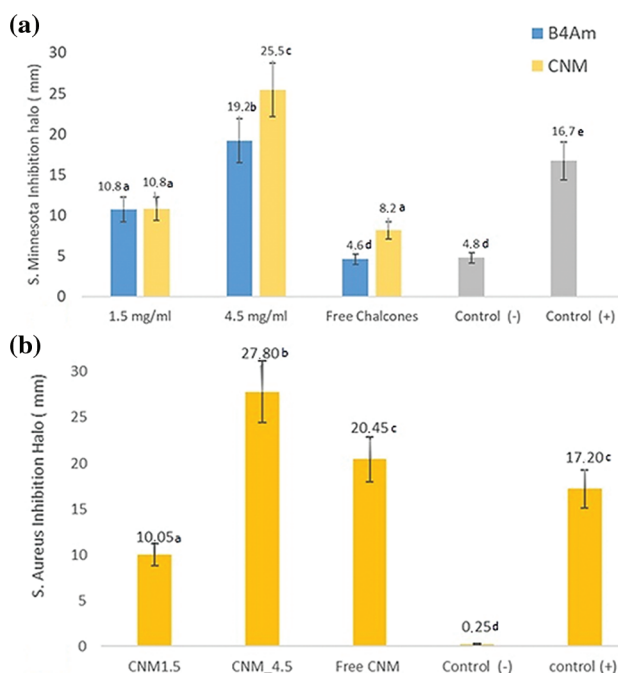


Figure 5: (a) Inhibition halo (mm) of free CNM and B4AM and nanoemulsions loaded at 1.5 and 4.5 mg/mL against *S. minnesota*; (b) Inhibition halo (mm) of free CNM, and CNM nanoemulsion loaded at 1.5 and 4.5 mg/mL against *S. aureus*. Empty nanoemulsion was used as a negative control and sulfamethoxazole + trimethoprim at 100 µg/mL as a positive control

The CNM substance showed a discreet inhibition halo of 8 mm against *S. minnesota*, representing a median inhibitory activity, and with an inhibition halo of 20 mm against *S. aureus*. The free chalcone B4AM showed low antimicrobial activity against both types of microorganisms. Nanoemulsions loaded with chalcones at the same concentration as free chalcones showed a distinct pattern (Fig. S2, Supplementary Materials). The nanoemulsions B4AM_1.5 and B4AM_4.5 showed inhibitory halos of 10.8 and 19.2 mm, respectively, representing an increase of 230% and 420% in the activity in comparison with the free chalcone B4AM (4.6 mm) against *S. minnesota*. The B4AM_4.5 nanoemulsion showed equivalence to the concentration of the positive control in the standard dosage (Bactrim 100 µg). CNM_1.5 and CNM_4.5 nanoemulsions showed a higher inhibitory activity than Free Chalcone, with values of 132% and 312%, respectively, against *S. Minnesota*. The CNM_4.5 nanoemulsion had an excellent inhibition halo even when compared to the positive control. These results show this nanoemulsion has a significant antimicrobial effect compared to free chalcones and positive controls. It can be stated that in the nanoemulsion, the formation of tiny droplets increased activity against *S. minnesota*, probably related to the ease of penetration into the cell tissue wall of microorganisms.

The nanoemulsions had their antimicrobial activity tested against *S. aureus* and the results of the inhibition zones measured in diameters are shown in Fig. 5b (Fig. S3, Supplementary Materials). In the halo of inhibition test against *S. aureus*, only CNM free chalcone and its nanoemulsions with CNM showed antimicrobial activity. Chalcones' antimicrobial effects are attributed to a strong unsaturated keto feature in the molecule [55]. Possibly, the greater number of conjugated bonds in CNM increased the antimicrobial activity in comparison with B4AM, especially against a resistant microorganism as *S. aureus*.

The nanoemulsion loaded with CNM at 4.5 mg/mL showed increased activity to 136% compared with the free chalcone, and an equivalence behavior compared to the positive control. In general, CNM_4.5 was

the best formulation of the nanoemulsions, because of the significant antimicrobial effect against the two types of microorganisms tested. One of the major factors that contributed to its microbial action is because of the formation of nanometric domains. As stated by Benjemaa et al. [56], the nanoization of a compound can increase the dissolution rate, wetting, particle surface area and saturation solubility, further highlighting the bioavailability because of the enhanced *in vivo* release, as only the solubilized particles are absorbed via the lipophilic cell membrane. Alginate contributed to the stability of nanoemulsions as it was at the droplet interface and formed a very thin layer of negative charge, preventing Ostwald maturation.

Regarding the *in vitro* antifungal activity of chalcones B4AMIN and CNM in its free form, results showed that B4AM presented inhibition halo (9.0 ± 1.0) and (7.7 ± 0.57) against *C. albicans* strains ATCC and LABMIC 0102, where Nystatin presented an inhibition halo of respectively 12.58 ± 0.35 and 14.33 ± 0.578 . On the other hand, CNM did not show inhibitory activity. These results agree with the literature. The fungal cell wall differs from the bacterial cell wall and is not affected by antibacterial cell wall inhibitors, where antifungal agents may contribute to the cell membrane disruption, inhibition of cell division or inhibition of cell wall formation [57]. Allylamine has effective activity against dermatophyte and is noncompetitive inhibitors of the first step in ergosterol biosynthesis [9]. In the study by Kozłowska et al. [58], the effect of structure of 18 amino-chalcones on the biological activity was revealed, where the presence of an amino group in the meta position with the addition of the aromatic ring in the compound, increased the hydrophobicity of the molecule, facilitating penetration of Chalcone into the cells of microorganisms.

The results from the minimum inhibitory concentration against *Candida albicans* are summarized in Table 3. Chalcone B4AM and nanoemulsions loaded with B4AM showed significant inhibitory activity when tested against two strains of *C. albicans* (ATCC 90028 and LABMIC 0102). Particularly, ALG_15B4AM, showed equivalent inhibitory capacity with three-fold lower chalcone content.

Table 3: Minimum inhibitory concentration (MIC) in mg.mL^{-1} of nanoemulsions against *C. albicans*. NI: no inhibition

Formulation	Chalcone content (mg.mL^{-1})	MIC ATCC (90028)	MIC 0102 (clinical)
ALG_15B4AM	1.5	0.350	0.175
ALG_45B4AM	4.5	0.625	0.312
B4AM	10.0	0.625	0.625
CNM	10.0	NI	NI
ALG (negative control)	—————	NI	NI
ANFOT. B (positive control)	—————	0.001	0.001

Their behavior was enhanced in comparison with free B4AM, showing the nanoemulsion loaded at 1.5 mg/mL presented improved fungistatic action in comparison with free DB4AM at a concentration of 10 mg/mL. In the literature, we did not find studies on nanoemulsions with chalcones against *C. albicans*, but we found the work of Medina-Alarcon et al. [32] who evaluated the antifungal activity of 2'-hydroxychalcone loaded in nanoemulsion against *Paracoccidioides* spp. and found an MIC of 0.06 $\mu\text{g/mL}$, thus showing a potential new alternative treatment for paracoccidioidomycosis. In our work we also found this potential for the treatment of infections caused by *Candida*, candidiasis. The different MICs were probably due to the fungal species used.

The association of nanostructures with bioactive compounds improves several characteristics, such as protection against degradation, solubility, stability, and bioavailability, among others [59]. B4AM is an allylamine, which suggests an action as a noncompetitive inhibitor of the first step in ergosterol biosynthesis [9]. This study showed that nanoemulsions with B4AM formed stable nanodroplets, favoring the solubilization of the chalcone in the oily phase and the formation of a fraction with tiny droplets (51.4 nm) favoring easy passive transport through the fungal cell membrane. As discussed in the literature, the nanometric size of the droplets increases bioavailability and enhances the diffusion because of the subcellular size [57].

4 Conclusion

This study showed that alginate nanoemulsions loaded with chalcones have high stability based on macroscopic and microscopic parameters. Particularly, the emulsions loaded with a dosage of 1.5 mg/mL showed long kinetic stability, preventing droplet aggregation and gravitational separation. The nanoemulsions were found to be nanometric in size, with polydisperse indexes that were low, equal to, or less than 200 nm. According to the antimicrobial inhibition test, nanoemulsions carrying B4AM displayed activity against *S. minnesota*, particularly the one with the highest dosage, with a 420% greater inhibitory response compared to the free form and equivalence to the positive control. Nanoemulsions loaded with CNM showed excellent inhibitory activity at the highest dosage, equivalent to the positive control against *S. minnesota* and *S. aureus*. B4AM was the only substance with an inhibition halo against *C. albicans*, probably by inhibition of cell wall formation. Nanoemulsions with B4AM with nanodroplets increased bioavailability and enhanced the diffusion because of the subcellular size, facilitating penetration of chalcone into the cells of microorganisms. As a result, CNM is a potential candidate with antibacterial action, and B4AM is a potential candidate with antifungal action. The nanoemulsions showed efficient micellization, favoring the solubilization of chalcones in the oil phase and the formation of tiny droplets with low PDI, with easy passive transport through the bacterial cell membrane, being promising for the development of new drugs.

Acknowledgement: The authors would like to thank the Northeastern Center for Application and Use of Nuclear Magnetic Resonance-CENAUREM-Brazil for the support in FTIR analysis.

Funding Statement: This study was supported by the National Council for Scientific Development-CNPQ/MCTI/FNDCT N18/2021, by the Concession of Research Funding Grant Number 406522/2021-9-1 to F. O. M. S. Abreu. Helcio Silva dos Santos acknowledges financial support from CNPq-PQ (Grant Number 306008/2022-0).

Author Contributions: The authors confirm contribution to the paper as follows: Study conception and design: F. O. M. S. Abreu, M. M. C. Forte; Data collection: J. F. do Nascimento, H. N. Pinheiro, F. R. S. Mendes, R. M. Castelo, T. Holanda, T. Benincá, J. C. S. Prado; Analysis and interpretation of results: F. O. M. S. Abreu, J. F. do Nascimento, R. M. Castelo, H. N. Pinheiro; M. M. C Forte, R. O. Fontenelle; Draft manuscript preparation: F. O. M. S. Abreu, J. F. do Nascimento, M. M. C Forte, P. S. Malheiros. All authors reviewed the results and approved the final version of the manuscript.

Availability of Data and Materials: The data that support the findings of this study are available from the corresponding author, (F. O. M. S. Abreu), upon reasonable request.

Conflicts of Interest: The authors declare that they have no conflicts of interest to report regarding the present study.

References

1. Ferrari, R. G., Rosario, D. K. A., Cunha-Neto, A., Mano, S. B., Figueiredo, E. E. S. et al. (2019). Worldwide epidemiology of *salmonella* serovars in animal-based foods: A meta-analysis. *Applied and Environmental Microbiology*, 85(14). <https://doi.org/10.1128/AEM.00591-19>
2. Saidenberg, A. B. S., Franco, L. S., Reple, J. N., Hounmanou, Y. M. G., Casas, M. R. T. et al. (2023). *Salmonella* Heidelberg and *Salmonella* Minnesota in Brazilian broilers: Genomic characterization of third-generation cephalosporin and fluoroquinolone-resistant strains. *Environmental Microbiology Reports*, 15(2), 119–128. <https://doi.org/10.1111/1758-2229.13132>
3. Hessel, C. T., de Freitas Costa, E., Boff, R. T., Pessoa, J. P., Tondo, E. C. (2022). A systematic review and Bayesian meta-analysis about *Salmonella* spp. prevalence on raw chicken meat. *Microbial Risk Analysis*, 21, 100205. <https://doi.org/10.1016/j.mran.2022.100205>
4. Cheung, G. Y. C., Bae, J. S., Otto, M. (2021). Pathogenicity and virulence of *Staphylococcus aureus*. *Virulence*, 12(1), 547–569. <https://doi.org/10.1080/21505594.2021.1878688>
5. Eze, F. U., Okoro, U. C., Ugwu, D. I., Okafor, S. N. (2019). Biological activity evaluation of some new benzenesulphonamide derivatives. *Frontiers in Chemistry*, 7, <https://doi.org/10.3389/fchem.2019.00634>
6. Soliman, S., Alnajdy, D., El-Keblawy, A., Mosa, K., Khoder, G. et al. (2017). Plants' natural products as alternative promising anti-Candida drugs. *Pharmacognosy Reviews*, 11(22), 104. https://doi.org/10.4103/phrev.phrev_8_17
7. Siqueira, L. B. D. O., Matos, A. P. D. S., Cardoso, V. D. S., Villanova, J. C. O., Guimarães, B. D. C. L. R. et al. (2019). Clove oil nanoemulsion showed potent inhibitory effect against *Candida* spp. *Nanotechnology*, 30(42), 425101. <https://doi.org/10.1088/1361-6528/ab30c1>
8. Fei, P., Ali, M. A., Gong, S., Sun, Q., Bi, X. et al. (2018). Antimicrobial activity and mechanism of action of olive oil polyphenols extract against *Cronobacter sakazakii*. *Food Control*, 94, 289–294. <https://doi.org/10.1016/j.foodcont.2018.07.022>
9. Zhang, Q. Y., Yan, Z. B., Meng, Y. M., Hong, X. Y., Shao, G. et al. (2021). Antimicrobial peptides: Mechanism of action, activity and clinical potential. *Military Medical Research*, 8(1), 48. <https://doi.org/10.1186/s40779-021-00343-2>
10. Rammohan, A., Reddy, J. S., Sravya, G., Rao, C. N., Zyryanov, G. V. (2022). Chalcone synthesis, properties and medicinal applications: A review. *Environmental Chemistry Letters*, 18(1), 433–458. <https://doi.org/10.1007/s10311-019-00959-w>
11. Okolo, E. N., Ugwu, D. I., Ezema, B. E., Ndefo, J. C., Eze, F. U. et al. (2021). New chalcone derivatives as potential antimicrobial and antioxidant agent. *Scientific Reports*, 11(1), 21781. <https://doi.org/10.1038/s41598-021-01292-5>
12. Shih, T. L., Liu, M. H., Li, C. W., Kuo, C. F. (2018). Halo-substituted chalcones and azachalcones inhibited lipopolysaccharite-stimulated pro-inflammatory responses through the TLR4-mediated pathway. *Molecules*, 23(3), 597. <https://doi.org/10.3390/molecules23030597>
13. Dan, W., Dai, J. (2020). Recent developments of chalcones as potential antibacterial agents in medicinal chemistry. *European Journal of Medicinal Chemistry*, 187, 111980. <https://doi.org/10.1016/j.ejmech.2019.111980>
14. Kuttithodi, A. M., Nikhitha, D., Jacob, J., Narayanankutty, A., Mathews, M. et al. (2022). Antioxidant, antimicrobial, cytotoxicity, and larvicidal activities of selected synthetic bis-chalcones. *Molecules*, 27(23), 8209. <https://doi.org/10.3390/molecules27238209>
15. Li, X., Wang, L., Wang, B. (2017). Optimization of encapsulation efficiency and average particle size of *Hohenbuehelia serotina* polysaccharides nanoemulsions using response surface methodology. *Food Chemistry*, 229, 479–486. <https://doi.org/10.1016/j.foodchem.2017.02.051>
16. Demisli, S., Mitsou, E., Pletsa, V., Xenakis, A., Papadimitriou, V. (2020). Development and Study of nanoemulsions and nanoemulsion-based hydrogels for the encapsulation of lipophilic compounds. *Nanomaterials*, 10(12), 2464. <https://doi.org/10.3390/nano10122464>

17. Guttoff, M., Saberi, A. H., McClements, D. J. (2015). Formation of vitamin D nanoemulsion-based delivery systems by spontaneous emulsification: Factors affecting particle size and stability. *Food Chemistry*, 171, 117–122. <https://doi.org/10.1016/j.foodchem.2014.08.087>
18. Aswathanarayan, J. B., Vittal, R. R. (2019). Nanoemulsions and their potential applications in food industry. *Frontiers in Sustainable Food Systems*, 3. <https://doi.org/10.3389/fsufs.2019.00095>
19. Schuh, R. S., Bruxel, F., Teixeira, H. F. (2014). Physicochemical properties of lecithin-based nanoemulsions obtained by spontaneous emulsification or high-pressure homogenization. *Química Nova*. <https://doi.org/10.5935/0100-4042.20140186>
20. Jamoussi, Y., Zaiter, T., Desrumaux, C., Acar, N., Pellequer, Y. et al. (2021). Investigation of the spontaneous nanoemulsification process with medium- and long-chain triglycerides. *Colloids and Surfaces B: Biointerfaces*, 197, 111432. <https://doi.org/10.1016/j.colsurfb.2020.111432>
21. Zhou, Y., Zhao, W., Lai, Y., Zhang, B., Zhang, D. (2020). Edible plant oil: Global status, health issues, and perspectives. *Frontiers in Plant Science*, 11, <https://doi.org/10.3389/fpls.2020.01315>
22. Wijekoon, M. M. J. O., Mahmood, K., Ariffin, F., Mohammadi Nafchi, A., Zulkurnain, M. (2023). Recent advances in encapsulation of fat-soluble vitamins using polysaccharides, proteins, and lipids: A review on delivery systems, formulation, and industrial applications. *International Journal of Biological Macromolecules*, 241, 124539. <https://doi.org/10.1016/j.ijbiomac.2023.124539>
23. Gahruie, H., Ziaee, E., Eskandari, M. H., Hosseini, S. M. H. (2017). Characterization of basil seed gum-based edible films incorporated with Zataria multiflora essential oil nanoemulsion. *Carbohydrate Polymers*, 166, 93–103. <https://doi.org/10.1016/j.carbpol.2017.02.103>
24. Abreu, F. O. M.da S., Costa, E. F., Cardial, M. R. L., André, W. P. P. (2020). Polymeric nanoemulsions enriched with Eucalyptus citriodora essential oil. *Polímeros*, 30(2). <https://doi.org/10.1590/0104-1428.00920>
25. Teixe-Roig, J., Oms-Oliu, G., Odriozola-Serrano, I., Martín-Belloso, O. (2022). Enhancing the gastrointestinal stability of curcumin by using sodium alginate-based nanoemulsions containing natural emulsifiers. *International Journal of Molecular Sciences*, 24(1), 498. <https://doi.org/10.3390/ijms24010498>
26. Maphosa, Y., Jideani, V. A. (2018). Factors affecting the stability of emulsions stabilised by biopolymers. In: *Science and technology behind nanoemulsions*. InTech. <https://doi.org/10.5772/intechopen.75308>
27. Nel, A. E., Mädler, L., Velegol, D., Xia, T., Hoek, E. M. V. et al. (2009). Understanding biophysicochemical interactions at the nano-bio interface. *Nature Materials*, 8(7), 543–557. <https://doi.org/10.1038/nmat244228>
28. Winter, E., Pizzol, C., Locatelli, C., Silva, A., Conte, A. et al. (2014). *In vitro* and *in vivo* effects of free and chalcones-loaded nanoemulsions: Insights and challenges in targeted cancer chemotherapies. *International Journal of Environmental Research and Public Health*, 11(10), 10016–10035. <https://doi.org/10.3390/ijerph111010016>
29. Mattos, C. B., Deponti, V. B., Barreto, F., Simões, C. M. O., Andrighetti-Frohner, C. R. et al. (2012). Development of a stability-indicating LC method for determination of a synthetic chalcone derivative in a nanoemulsion dosage form and identification of the main photodegradation product by LC-MS. *Journal of Pharmaceutical and Biomedical Analysis*, 70, 652–656. <https://doi.org/10.1016/j.jpba.2012.07.021>
30. Coelho, D., Veleirinho, B., Mazzarino, L., Alberti, T., Buzanello, E. et al. (2021). Polyvinyl alcohol-based electrospun matrix as a delivery system for nanoemulsion containing chalcone against *Leishmania (Leishmania) amazonensis*. *Colloids and Surfaces B: Biointerfaces*, 198, 111390. <https://doi.org/10.1016/j.colsurfb.2020.111390>
31. Leal, A. L. A. B., Silva, P. T., Rocha, M. N., Marinho, E. M., Marinho, E. S. et al. (2021). Potentiating activity of Norfloxacin by synthetic chalcones against NorA overproducing *Staphylococcus aureus*. *Microbial Pathogenesis*, 155, 104894. <https://doi.org/10.1016/j.micpath.2021.104894>
32. Medina-Alarcón, K. P., Singulani, J. L., Dutra, L. A., Pitanguí, N. S., Pereira-da-Silva, M. A. et al. (2020). Antifungal activity of 2'-hydroxychalcone loaded in nanoemulsion against *Paracoccidioides* spp. *Future Microbiology*, 15(1), 21–33. <https://doi.org/10.2217/fmb-2019-0095>
33. Romeu, M. C., Freire, P. T. C., Ayala, A. P., Barreto, A. C. H., Oliveira, L. S. et al. (2022). Synthesis, crystal structure, ATR-FTIR, FT-Raman and UV spectra, structural and spectroscopic analysis of (3E)-4-[4-

- (dimethylamine)phenyl]but-3-en-2-one. *Journal of Molecular Structure*, 1264, 133222. <https://doi.org/10.1016/j.molstruc.2022.133222>
34. CLSI M27-A3 (2008). Reference method for broth dilution antifungal susceptibility testing of yeasts. *Approved Standard*. Clinical and Laboratory Standards Institute, Wayne, PA, USA. <https://www.clsi.org/1-56238-666-2> (accessed on 03/05/2022)
 35. Kim, Y. J., Lee, K. P., Lee, D. Y., Kim, Y. T., Koh, D. et al. (2019). Anticancer activity of a new chalcone derivative-loaded polymeric micelle. *Macromolecular Research*, 27(1), 48–54. <https://doi.org/10.1007/s13233-019-7002-y>
 36. Paiva, J. C. F., Morais, S. M., Sobrinho, A. C. N., Cavalcante, G. S., Silva, N. A. et al. (2019). Design of chitosan-alginate core-shell nanoparticles loaded with anacardic acid and cardol for drug delivery. *Polímeros*, 29(4). <https://doi.org/10.1590/0104-1428.08118>
 37. Oliveira, E. F., Paula, H. C. B., de Paula, R. C. M. (2014). Alginate/cashew gum nanoparticles for essential oil encapsulation. *Colloids and Surfaces B: Biointerfaces*, 113, 146–151. <https://doi.org/10.1016/j.colsurfb.2013.08.038>
 38. Abreu, F. O. M. S., Bianchini, C., Forte, M. M. C., Kist, T. B. L. (2008). Influence of the composition and preparation method on the morphology and swelling behavior of alginate-chitosan hydrogels. *Carbohydrate Polymers*, 74(2), 283–289. <https://doi.org/10.1016/j.carbpol.2008.02.017>
 39. Rohman, A., Setyaningrum, D. L., Riyanto, S. (2014). FTIR spectroscopy combined with partial least square for analysis of red fruit oil in ternary mixture system. *International Journal of Spectroscopy*, 2014(1), 1–5. <https://doi.org/10.1155/2014/785914>
 40. Joseph, L., Sajan, D., Shettigar, V., Chaitanya, K., Misra, N. et al. (2013). Synthesis, crystal growth, thermal studies and scaled quantum chemical studies of structural and vibrational spectra of the highly efficient organic NLO crystal: 1-(4-Aminophenyl)-3-(3,4-dimethoxyphenyl)-prop-2-en-1-one. *Materials Chemistry and Physics*, 141(1), 248–262. <https://doi.org/10.1016/j.matchemphys.2013.05.007>
 41. Santiago, R. N. S., Freire, P. T. C., Teixeira, A. M. R., Bandeira, P. N., Santos, H. S. et al. (2018). FT-Raman and FT-IR spectra and DFT calculations of chalcone (2E)-1-(4-aminophenyl)-3-phenyl-prop-2-en-1-one. *Vibrational Spectroscopy*, 97, 1–7. <https://doi.org/10.1016/j.vibspec.2018.04.007>
 42. Custodio, J. M. F., Vaz, W. F., Andrade, F. M., Camargo, A. J., Oliveira, G. R. et al. (2017). Substitution effect on a hydroxylated chalcone: Conformational, topological and theoretical studies. *Journal of Molecular Structure*, 1136, 69–79. <https://doi.org/10.1016/j.molstruc.2017.01.076>
 43. McClements, D. J. (2010). Emulsion design to improve the delivery of functional lipophilic components. *Annual Review of Food Science and Technology*, 1(1), 241–269. <https://doi.org/10.1146/annurev.food.080708.100722>
 44. Salvia-Trujillo, L., Decker, E. A., McClements, D. J. (2016). Influence of an anionic polysaccharide on the physical and oxidative stability of omega-3 nanoemulsions: Antioxidant effects of alginate. *Food Hydrocolloids*, 52, 690–698. <https://doi.org/10.1016/j.foodhyd.2015.07.035>
 45. Dickinson, E. (2009). Hydrocolloids as emulsifiers and emulsion stabilizers. *Food Hydrocolloids*, 23(6), 1473–1482. <https://doi.org/10.1016/j.foodhyd.2008.08.005>
 46. Chanamai, R., McClements, D. J. (2000). Creaming stability of flocculated monodisperse oil-in-water emulsions. *Journal of Colloid and Interface Science*, 225(1), 214–218. <https://doi.org/10.1006/jcis.2000.6766>
 47. Abu Ali, O. A., El-Naggar, M. E., Abdel-Aziz, M. S., Saleh, D. I., Abu-Saied, M. A. et al. (2021). Facile synthesis of natural anise-based nanoemulsions and their antimicrobial activity. *Polymers*, 13(12), 2009. <https://doi.org/10.3390/polym13122009>
 48. Hassanshahian, M., Saadatfar, A., Masoumpour, F. (2020). Formulation and characterization of nanoemulsion from Alhagi maurorum essential oil and study of its antimicrobial, antibiofilm, and plasmid curing activity against antibiotic-resistant pathogenic bacteria. *Journal of Environmental Health Science and Engineering*, 18(2), 1015–1027. <https://doi.org/10.1007/s40201-020-00523-7>
 49. Islam, M. A., Barua, S., Barua, D. (2017). A multiscale modeling study of particle size effects on the tissue penetration efficacy of drug-delivery nanoparticles. *BMC Systems Biology*, 11(1), 113. <https://doi.org/10.1186/s12918-017-0491-4>

50. Bandi, S. P., Kumbhar, Y. S., Venuganti, V. V. K. (2020). Effect of particle size and surface charge of nanoparticles in penetration through intestinal mucus barrier. *Journal of Nanoparticle Research*, 22(3), 62. <https://doi.org/10.1007/s11051-020-04785-y>
51. Kentish, S., Wooster, T. J., Ashokkumar, M., Balachandran, S., Mawson, R. et al. (2008). The use of ultrasonics for nanoemulsion preparation. *Innovative Food Science & Emerging Technologies*, 9(2), 170–175. <https://doi.org/10.1016/j.ifset.2007.07.005>
52. Sneha, K., Kumar, A. (2022). Nanoemulsions: Techniques for the preparation and the recent advances in their food applications. *Innovative Food Science & Emerging Technologies*, 76, 102914. <https://doi.org/10.1016/j.ifset.2021.102914>
53. Liu, W., Sun, D., Li, C., Liu, Q., Xu, J. (2006). Formation and stability of paraffin oil-in-water nano-emulsions prepared by the emulsion inversion point method. *Journal of Colloid and Interface Science*, 303(2), 557–563. <https://doi.org/10.1016/j.jcis.2006.07.055>
54. Mattos, C. B., Argenta, D. F., Melchiades, G. D. L., Cordeiro, M. N. S., Tonini, M. L. et al. (2015). Nanoemulsions containing a synthetic chalcone as an alternative for treating cutaneous leishmaniasis: Optimization using a full factorial design. *International Journal of Nanomedicine*, 10, 5529–5542. <https://doi.org/10.2147/IJN.S83929>
55. Babu, A. K., Selvaraju, K. (2022). Synthesis, biological evaluation and docking studies of novel chalcone derivatives as antimicrobial agents. *Materials Today: Proceedings*, 48, 382–386. <https://doi.org/10.1016/j.matpr.2020.09.551>
56. Benjemaa, M., Neves, M. A., Falleh, H., Isoda, H., Ksouri, R. et al. (2018). Nanoencapsulation of Thymus capitatus essential oil: Formulation process, physical stability characterization and antibacterial efficiency monitoring. *Industrial Crops and Products*, 113, 414–421. <https://doi.org/10.1016/j.indcrop.2018.01.062>
57. Krishnamoorthy, R., Gassem, M. A., Athinarayanan, J., Periyasamy, V. S., Prasad, S. et al. (2021). Antifungal activity of nanoemulsion from Cleome viscosa essential oil against food-borne pathogenic Candida albicans. *Saudi Journal of Biological Sciences*, 28(1), 286–293. <https://doi.org/10.1016/j.sjbs.2020.10.001>
58. Kozłowska, J., Potaniec, B., Baczyńska, D., Żarowska, B., Anioł, M. (2019). Synthesis and biological evaluation of novel aminochalcones as potential anticancer and antimicrobial agents. *Molecules*, 24(22), 4129. <https://doi.org/10.3390/molecules24224129>
59. Bazana, M. T., Codevilla, C. F., de Menezes, C. R., (2019). Nanoencapsulation of bioactive compounds: Challenges and perspectives. *Current Opinion in Food Science*, 26, 47–56. <https://doi.org/10.1016/j.cofs.2019.03.005>

Supplementary Materials

Table S1: ANOVA – Influence of the parameters on the particle size. Factor A: Chalcone dosage; Factor B: chalcone type. $p < 0.05$. SQ – Sum of Quares; DF – Degree of freedom; MS – Median square; Fo – Calculated F value; Fc – Statistical F value for comparison. When Fo is higher than Fc, then the factor is significant. p -value < 0.05

	SQ	DF	MS	Fo	Fcritical
Factor A	26439.4	1	26439.42	33.98	5.318
Factor B	1579.0	1	1578.96	2.03	5.318
Interaction A \times B	1934.2	1	1934.21	2.49	5.318
Residue	6225.4	8	778.17		
Total	36178.0	11			

Table S2: ANOVA – Influence of the parameters on the zeta size. Factor A: Chalcone dosage; Factor B: chalcone type. $p < 0.05$. SQ – Sum of Quares; DF – Degree of freedom; MS – Median square; Fo – calculated F value; Fc – statistical F value for comparison. When Fo is higher than Fc, then the Factor is significant. p -value < 0.05

	SQ	GL	MQ	Fo	Fcritical
Factor A	142.83	1	142.83	71.18	5.318
Factor B	79.05	1	79.05	39.39	5.318
Interaction A \times B	2.25	1	2.253	1.123	5.318
Residue	16.05	8	2.006		
Total	240.19	11			

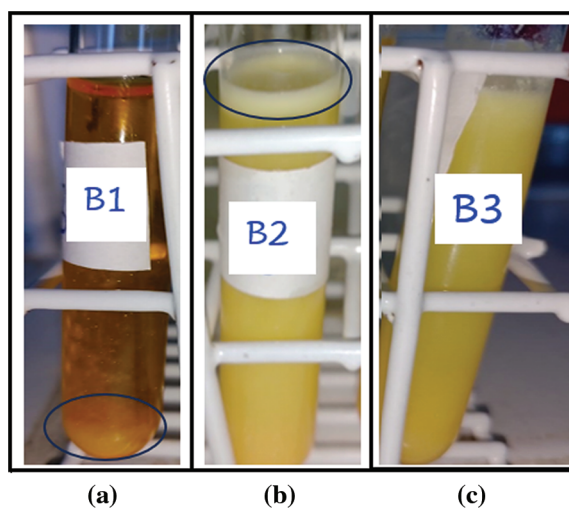


Figure S1: Stability of the nanoemulsions after seven days as a function of the composition of the system. (a) Nanoemulsion B1 (water, tween and chalcone B4AM) with significant signs of sedimentation and flocculation; (b) Nanoemulsion B2 (water, tween, soybean oil and chalcone B4AM) with significant creaming formation; (c) Nanoemulsion B3 (water, tween, soybean oil and ALG) with minimal sign of creaming and no evidence of sedimentation and flocculation

Table S3: Preliminary study regarding stability of nanoemulsion with tween, tween plus soybean oil and tween, soybean oil and ALG after seven days

	Components	Signs of instability
Tw_B4M (B1)	Tween	Sedimentation (+++) Floculation (+++)
Tw_Os_B4M (B2)	Soybean oil + Tween	Creaming (+++)
Tw_Os_ALG_B4M (B3)	Soybean oil + Tween + ALG	Creaming (+)

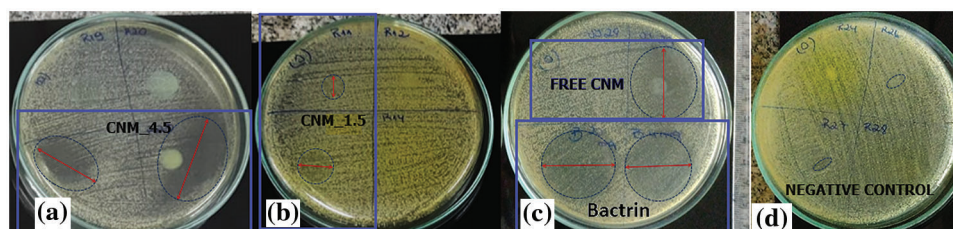


Figure S2: Inhibition halo of positive control, negative control and the nanoemulsions against *S. aureus*

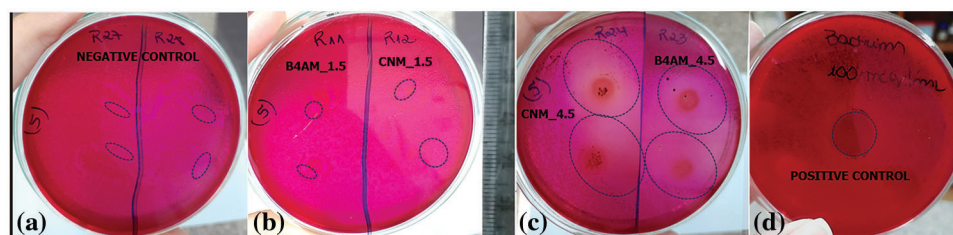


Figure S3: Inhibition halo of negative control (a), nanoemulsions loaded with chalcones at 1.5 mg/ml (b), nanoemulsions loaded with chalcones at 4.5 mg/ml (c) and positive control against *S. minnesota* (d)